

EVENT-TRIGGERED BASED MODEL-FREE ADAPTIVE SLIDING MODE CONSTRAINED CONTROL FOR NONLINEAR DISCRETE-TIME SYSTEMS

CHUANWEN GAO, WEIMING ZHANG*, DEZHI XU, WEILIN YANG
AND TINGLONG PAN

School of Internet of Things Engineering
Jiangnan University
No. 1800, Lihu Avenue, Wuxi 214122, P. R. China
6191915010@stu.jiangnan.edu.cn; { xudezhi; wlyang; tlpan }@jiangnan.edu.cn
*Corresponding author: wmzhang@stu.jiangnan.edu.cn

Received August 2021; revised November 2021

ABSTRACT. *In this paper, a novel model-free adaptive event-triggered control strategy is proposed for nonlinear discrete-time systems. Firstly, the nonlinear system is described as an equivalent linear model via the compact form dynamic linearization method, and the pseudo partial derivative is estimated based on an observer-based adaptive law. Then, the anti-windup compensator is used to settle out the actuator saturation phenomenon in the control system, and the equivalent control law and switching control law are designed to track the desired output signal. Considering the computational pressure and time cost, the event-triggered mechanism is designed, which only updates the control signal when the preset event triggering condition is satisfied, and the stability of the proposed control algorithm is justified. Finally, the validity and applicability of the control strategy are verified by a simulation example.*

Keywords: Event-triggered control, Model-free adaptive control, Sliding mode constrained control, Discrete-time nonlinear systems

1. Introduction. With the increasing complexity of production process and technology, the working principle of industrial process system becomes more complex, which makes it more difficult to describe the dynamic behavior and establish the accurate mathematical model. Hence, model-free control methods are gradually proposed to make up for the powerless status of model-based control methods in solving such problems. Model-free adaptive control (MFAC) was first put forward by Hou in 1994, and has achieved a wealth of theoretical results and a wide range of practical applications in recent years [1-11]. MFAC does not need to acquire any model information of the controlled object, and only relies on the system output and control input data to execute the controller design process [1].

Most MFAC algorithms are designed based on real-time sampling, which may sacrifice computing costs in search of better performance [12]. Event-triggered control (ETC) technology has received increasing attention in recent years due to its advantages in saving network resources and less calculation costs [13]. The controllers in ETC strategies only perform the calculations when the preset conditions are triggered. In terms of the event-triggered mechanism, it can be divided into relative threshold type and fixed threshold type. The relative threshold type is related to the system state, which can achieve more accurate control and help to achieve the balance between communication resource

utilization and system performance, while the fixed threshold type can be considered as a special case of relative threshold type [12-19].

For the purposes of saving network resources and reducing calculation burden, some researches have been accomplished in the fields of MFAC and ETC. In [12], the event-triggered MFAC algorithms were designed based on various dynamic linearization methods, which explored the event triggering mechanisms of various data-driven models. In terms of improving the degree of intelligence, an event-based MFAC algorithm is proposed with neural network technique in [13]. Besides, a novel event-triggered mechanism by combining ETC with robust fuzzy control is designed in [15]. When it comes to different application environments, an event-based MFAC method is applied to the disturbed system to improve the utilization of network communication resources in [16], and the packet dropout issues are studied in [17] by designing the event-triggered MFAC method with packet dropout compensation algorithm. In general, the aforementioned work explores the feasibility of ETC in MFAC, but few studies achieve the balance between control performance and calculation costs, and the saturation problem has not been discussed in this condition.

Motivated by the above analysis, a novel event-triggered based model-free adaptive sliding mode constrained control method is proposed in this paper. The actuator saturation problem is handled by introducing an anti-windup compensator to the proposed sliding mode constrained control strategy, which ensures the robustness and performance of the control system. Meanwhile, an event-triggered mechanism is presented and integrated into the proposed control strategy, and the system stability is analyzed at different conditions (event-triggered instants and inter-events instants).

Different from the traditional MFAC algorithm which calculates the control signal at a fixed sampling time, the proposed algorithm only updates the control signal when the event-triggered error satisfies the designed condition. In addition, the event-triggered mechanism and event-triggered error proposed in this paper are designed according to the system output data; therefore, the control performance on system output and calculation costs can be balanced by adjusting the preset event-triggered parameter. The introduction of event triggering greatly reduces the computational burden based on the original control performance of MFAC, so our method makes both available. By the way, compared with the ETC strategies using neural network or fuzzy control, the controller is easier to implement and the structure of the proposed scheme is simpler.

The rest of this paper is organized as follows. Section 2 establishes data-driven model of the nonlinear system via the compact form dynamic linearization (CFDL) method and observer-based pseudo partial derivative (PPD) estimation algorithm. Then, the sliding mode constrained control strategy integrated with event-triggered mechanism is proposed in Section 3 including the stability analysis. After that, the proposed control method has application in a simulation example to verify its feasibility in Section 4. Finally, Section 5 shows some conclusions drawn from the study.

2. Preliminaries.

2.1. CFDL-based data-driven model. Consider the following single input and single output (SISO) discrete-time nonlinear system:

$$y(k+1) = f(y(k), \dots, y(k-n_y), u(k), \dots, u(k-n_u)) \quad (1)$$

where $y(k) \in R$, $u(k) \in R$, represent the system output and control input signal respectively, $f(\cdot \dots \cdot)$ is an unknown nonlinear function, and n_y and n_u are two unknown positive integers.

Assumption 2.1. *The partial derivative of $f(\cdot \cdot \cdot)$ respect to the control signal $u(k)$ is continuous [1].*

Assumption 2.2. *The nonlinear system (1) is generalized Lipschitz, i.e., $\forall k \geq 0, |\Delta y(k+1)| \leq \rho |\Delta u(k+1)|$ is established as long as $\Delta u(k) \neq 0$, where $\Delta u(k+1) = u(k+1) - u(k)$, $\Delta y(k+1) = y(k+1) - y(k)$, and $\rho > 0$ is a normal number [1].*

Lemma 2.1. *For the given nonlinear system (1), there must exist a PPD parameter $\phi(k)$ if Assumptions 2.1 and 2.2 hold, such that system (1) can be changed to the equivalent CFDL description only if $\Delta u(k) \neq 0$ as follows [1]:*

$$\Delta y(k+1) = \phi(k)\Delta u(k) \tag{2}$$

where $\phi(k)$ satisfies $|\phi(k)| \leq m$, and m is a positive constant.

Proof: Detailed proof can be seen in [1].

2.2. Observer based PPD parameter identification. Since the value of PPD cannot be obtained directly, the observer based estimation algorithm has application in estimating PPD online [2]. Firstly, the structure of the output observer is designed as follows:

$$\hat{y}(k+1) = \hat{\phi}(k)\Delta u(k) + K_o e_o(k) + \hat{y}(k) \tag{3}$$

where $\hat{y}(k)$ represents the estimated value of the output, $e_o(k) = y(k) - \hat{y}(k)$ is the estimated error of $y(k)$, $\hat{\phi}(k)$ represents the estimated value of PPD, and K_o is the undetermined observer gain. Combining (2) with (3), the dynamic characteristic of $e_o(k)$ is defined as

$$e_o(k+1) = \hat{\phi}(k)\Delta u(k) + \alpha e_o(k) \tag{4}$$

where $\hat{\phi}(k) = \phi(k) - \hat{\phi}(k)$ represents the PPD estimation error. $\alpha = 1 - K_o$ is the coefficient of the observer error, and satisfies $-1 < \alpha < 1$. Then, the update law of PPD is designed as

$$\hat{\phi}(k+1) = \Gamma(k)\Delta u(k)(e_o(k+1) - \alpha e_o(k)) + \hat{\phi}(k) \tag{5}$$

where $\Gamma(k) = 2(\mu + \Delta u^2(k))^{-1}$, and μ is a positive constant which is used to limit the change of PPD.

Remark 2.1. *A reset mechanism is introduced in this paper so as to ensure the tracking ability of PPD for time-variant parameters, which is defined as [1]*

$$\text{if } |\Delta u(k)| \leq \varepsilon \text{ or } \left| \hat{\phi}(k) \right| \leq \varepsilon \text{ or } \text{sign} \left(\hat{\phi}(k) \right) \neq \text{sign} \left(\hat{\phi}(1) \right), \quad \hat{\phi}(k) = \hat{\phi}(1) \tag{6}$$

where ε is a positive constant, $\text{sign}(\cdot)$ is symbolic function, and $\hat{\phi}(1)$ is the initial value of PPD estimation.

Lemma 2.2. *Comprehensively consider Equations (2)-(5), and it can be ensured that both $e_o(k)$ and $\hat{\phi}(k)$ keep boundedness for all k , that is, $\lim_{k \rightarrow \infty} [e_o(k), \hat{\phi}(k)] = [0, 0]$.*

Proof: Detailed proof is given in [2].

Since the value of $e_o(k+1)$ cannot be obtained at step k , a two-step delay uncertainty estimation technique is introduced to estimate $e_o(k+1)$ [3]. In combination with the observer (3), the system output at step $(k+1)$ can be obtained as

$$y(k+1) = \hat{\phi}(k)\Delta u(k) + (2 + K_o)e_o(k) - e_o(k-1) + \hat{y}(k) \tag{7}$$

So far, the CFDL linearization process and observer-based PPD estimation algorithm of the system are completed, which lays a foundation for the design of the controller.

3. Controller Design.

3.1. Sliding mode constrained control algorithm. In this part, the sliding mode constrained adaptive control algorithm is designed according to the above preliminary information. Sliding mode control (SMC) has strong robustness and is not affected by system parameter changes and external disturbances. It has been widely used in systems with high requirements for control accuracy [20]. On account of the above advantages, SMC is introduced in this paper. At the beginning of this section, the system tracking error is defined as

$$e(k) = y^*(k) - y(k) - \theta(k) \quad (8)$$

where $\theta(k)$ is the compensation signal, and $y^*(k)$ indicates the reference signal.

After that, the sliding mode surface is acquired from $e(k)$ as

$$s(k) = \lambda e(k) \quad (9)$$

where $\lambda > 0$ is the sliding mode gain.

To figure out the problem of actuator saturation which often occurs in control system, the anti-windup compensator is introduced in this paper [3]. It can solve the problems of actuator saturation and integral saturation in the control system [21]. These saturation phenomena will cause inestimable damage to the system.

When the controller is designed, the actuator saturation is simulated by imposing amplitude and rate constraints on the system input [22]. For system (1), define its amplitude constraint as

$$u_{\min} < u(k) < u_{\max} \quad (10)$$

where u_{\min} , u_{\max} represent the minimum and maximum of $u(k)$ respectively. And the constraint of control signal rate is defined as

$$\tilde{u}_{\min} < \tilde{u}(k) < \tilde{u}_{\max} \quad (11)$$

where $\tilde{u}(k) = \Delta u(k)/T_s$ represents the rate of $u(k)$, and \tilde{u}_{\min} , \tilde{u}_{\max} represent the minimum and maximum of $\tilde{u}(k)$ respectively.

Considering the above two constraints, the restricted control signal is as follows:

$$u(k) = \text{Sat}\{\text{Sat}\{u_o(k) - u(k-1), T_s \tilde{u}_{\min}, T_s \tilde{u}_{\max}\} + u(k-1), u_{\min}, u_{\max}\} \quad (12)$$

where $\text{Sat}(\cdot)$ is the limiting function, and $u_o(k)$ will be defined later.

Then, the dynamic characteristic of $\theta(k)$ is defined as follows:

$$\theta(k+1) = \hat{\phi}(k)(u_o(k) - u(k)) + \beta\theta(k) \quad (13)$$

where $\beta \in (0, 1)$ is the gain coefficient of compensation signal.

Remark 3.1. Suppose that $u_o(k) - u(k)$ is bounded. Due to the boundedness of $\hat{\phi}(k)$ and $0 < \beta < 1$, according to the stability criterion in [23], $\theta(k)$ is ultimately uniformly bounded (UUB).

On account of the basic concept of SMC, the following equivalent control law is used to keep the system state on sliding surface:

$$u_{eq}(k) = \frac{\hat{\phi}(k)}{\hat{\phi}^2(k) + \sigma} ((1 - \beta)\theta(k) + e_o(k-1) - (1 + K_o)e_o(k)) \quad (14)$$

where σ is a small normal number.

The switching control law is introduced here so as to ensure the control performance of equivalent control which is defined as [3]

$$u_{sw}(k) = \frac{\hat{\phi}(k)}{\hat{\phi}^2(k) + \sigma} \cdot \frac{\omega T_s \text{sign}(s(k)) + K_f T_s s(k)}{\lambda} \tag{15}$$

where $\omega > 0$ is switching factor, $K_f > 0$ is convergence coefficient, and $T_s > 0$ is the system sampling time.

To sum up, $u_o(k)$ is designed as

$$u_o(k) = u_{eq}(k) + u_{sw}(k) + u(k - 1) \tag{16}$$

The subsequent design of event-triggered controller will be based on these contents.

3.2. Event-triggered based controller design and stability analysis.

3.2.1. *Controller design.* Firstly, the event-triggered mechanism is designed as

$$k_{i+1} = k_i + \min_{\delta} \{ \delta \in N^+ \mid |y(k_i + \delta) - y(k_i)| \geq \xi \} \tag{17}$$

where $k_i, i = 1, 2, \dots$ are the event-triggered instants, and $\xi > 0$ is the given event-triggered parameter.

Then, the event-triggered error $e^{ET}(k)$ is obtained on the basis of system output data as follows:

$$e^{ET}(k) = y(k) - \bar{y}(k) \tag{18}$$

where $\bar{y}(k)$ represents the system output at the last event-triggered time, and it could be expressed as

$$\bar{y}(k) = y(k_i), \quad k_i \leq k < k_{i+1} \tag{19}$$

From (17) and (18), the event-triggered condition is defined as follows:

$$|e^{ET}(k)| \geq \xi \tag{20}$$

It can be concluded from the event-triggered mechanism that whether the event is triggered or not relies on the system output data and the preset event-triggered parameter.

Consider the above sliding mode constrained control algorithm, the event-triggered based controller structure is expressed as

$$\begin{cases} u_o(k) = \begin{cases} u(k - 1) + u_{eq}(k) + u_{sw}(k), & k = k_i \\ u(k - 1), & k \in (k_i, k_{i+1}) \end{cases} \\ u(k) = \text{Sat}\{(\text{Sat}\{u_o(k) - u(k - 1), T_s \tilde{u}_{\min}, T_s \tilde{u}_{\max}\}) + u(k - 1), u_{\min}, u_{\max}\} \end{cases} \tag{21}$$

In addition, the event-triggered factor $\gamma(k)$ is defined to record the trigger times:

$$\gamma(k) = \begin{cases} 1, & k = k_i \\ 0, & k \in (k_i, k_{i+1}) \end{cases} \tag{22}$$

3.2.2. Stability analysis.

Theorem 3.1. *Considering the nonlinear discrete-time SISO system (1) with Assumptions 2.1 and 2.2, the proposed control strategy guarantees the tracking error $e(k)$ satisfies UUB by choosing the appropriate parameters.*

Proof:

Case I: At the instant the event is triggered, i.e., $k = k_i$.

According to the controller, the sliding mode surface can be further expressed as

$$\begin{aligned} s(k_{i+1}) &= \Delta s(k_{i+1}) + s(k_i) \\ &= \lambda \left(E_o(k_i) - \frac{\hat{\phi}^2(k_i)}{\hat{\phi}^2(k_i) + \sigma} E_o(k_i) - \hat{\phi}(k_i) u_{sw}(k_i) \right) + s(k_i) \end{aligned} \tag{23}$$

$$= \left(1 - \frac{\hat{\phi}^2(k_i)}{\hat{\phi}^2(k_i) + \sigma} \cdot K_f T_s \right) s(k_i) + \Omega(k_i)$$

where $E_o(k_i)$ and $\Omega(k_i)$ are the defined intermediate variables as follows:

$$\begin{aligned} E_o(k_i) &= e_o(k_{i-1}) - (1 + K_o)e_o(k_i) + (1 - \beta)\theta(k_i) \\ \Omega(k_i) &= \frac{\lambda\sigma}{\hat{\phi}^2(k_i) + \sigma} E_o(k_i) - \frac{\hat{\phi}^2(k_i)}{\hat{\phi}^2(k_i) + \sigma} \omega T_s \text{sign}(s(k_i)) \end{aligned}$$

It can be seen from Lemma 2.2 and Remark 3.1 that $E_o(k_i)$ is bounded. Combined with the properties of symbolic function, $\Omega(k_i)$ is also bounded. Here, we suppose that $E_o(k_i) \leq E_o^M$ and $\Omega(k_i) \leq \Omega_M$, E_o^M and Ω_M are normal numbers.

Substituting the sliding mode surface (9) into (23), the following relationship can be obtained:

$$e(k_{i+1}) = \left(1 - \frac{\hat{\phi}^2(k_i)}{\hat{\phi}^2(k_i) + \sigma} \cdot K_f T_s \right) e(k_i) + \frac{\Omega(k_i)}{\lambda} \quad (24)$$

Based on the boundedness of $\Omega(k_i)$ and the reset mechanism in Remark 2.1, Equation (24) can be further expressed as

$$\begin{aligned} |e(k_{i+1})| &= \left(1 - \frac{\hat{\phi}^2(k_i)}{\hat{\phi}^2(k_i) + \sigma} \cdot K_f T_s \right) |e(k_i)| + \left| \frac{\Omega(k_i)}{\lambda} \right| \\ &\leq \left(\frac{(1 - K_f T_s)\varepsilon^2 + \sigma}{\varepsilon^2 + \sigma} \right) |e(k_i)| + \left| \frac{\Omega_M}{\lambda} \right| \end{aligned} \quad (25)$$

Select the appropriate K_f and T_s to make $0 < K_f T_s < 1$ hold, and the coefficient term can satisfy $0 < ((1 - K_f T_s)\varepsilon^2 + \sigma)/(\varepsilon^2 + \sigma) < 1$. Hence, it could be obtained according to Lemma 1 in [3] that

$$\lim_{k \rightarrow \infty} |e(k_i)| \leq \frac{(\varepsilon^2 + \sigma)\Omega_m}{\lambda K_f T_s} \quad (26)$$

When λ is large enough and σ is small enough, $\lim_{k \rightarrow \infty} |e(k_i)| = 0$ can be inferred, i.e., the system error satisfies UUB at the event-triggered instants $k = k_i$.

Case II: The instants between two adjacent trigger times, i.e., $k \in (k_i, k_{i+1})$.

According to the derivation above, $e(k+1)$ can be expressed as follows at these moments:

$$\begin{aligned} e(k+1) &= y^*(k+1) - y(k+1) - \theta(k+1) \\ &= y^*(k+1) - (e^{ET}(k) + y(k_i) + (1 + K_o)e_o(k) - e_o(k-1)) - \beta\theta(k) \\ &= \Delta y^*(k_i) + e(k_i) - e^{ET}(k) - \Lambda(k) \end{aligned} \quad (27)$$

where $\Delta y^*(k_i) = y^*(k+1) - y^*(k_i)$ and $\Lambda(k) = \beta\theta(k) - \theta(k_i) + (1 + K_o)e_o(k) - e_o(k-1)$.

In this paper, the given reference signal $y^*(k)$ is bounded by default, i.e., $y^*_m \leq y^*(k) \leq y^*_M$, such that $|\Delta y^*(k_i)| \leq \Delta y^*_M$, where $\Delta y^*_M = y^*_M - y^*_m \geq 0$. Based on Lemma 2.2 and Remark 3.1, $\Lambda(k)$ is bounded, i.e., $|\Lambda(k)| \leq \Lambda_M$, Λ_M is a positive constant.

In addition, considering the event triggered condition (20), the event-triggered errors satisfy $|e^{ET}(k)| < \xi$ during the inter-event times. Therefore, the following equation can be deduced from (27):

$$|e(k+1)| \leq |e(k_i)| + |e^{ET}(k)| + |\Lambda(k)| + |\Delta y^*(k_i)| < \xi + \Lambda_M + |e(k_i)| + \Delta y^*_M \quad (28)$$

It has been proved in the Case I that $\lim_{k \rightarrow \infty} |e(k_i)| \leq (\varepsilon^2 + \sigma)\Omega_m/\lambda K_f T_s = I$; therefore, the following equation can be obtained from (28):

$$\lim_{k \rightarrow \infty} |e(k)| = \lim_{k \rightarrow \infty} |e(k+1)| < E_M \quad (29)$$

where $E_M = \Delta y^*_M + \xi + \Lambda_M + I$ is a positive constant.

By choosing appropriate parameters and reference signal, $\lim_{k \rightarrow \infty} |e(k)| = 0$ could be deduced, i.e., $e(k)$ satisfies UUB for the instants $k \in (k_i, k_{i+1})$.

Considering discussion results of Case I and Case II together, Theorem 3.1 holds. \square

4. Simulation Analysis. A SISO nonlinear plant is described as [12]

$$y(k+1) = x_1(k) \frac{0.1 + y(k-1)}{1 + y(k-1)^2} + x_2(k)(y(k) + 1)u(k) + x_3(k)u(k-1)^3 \quad (30)$$

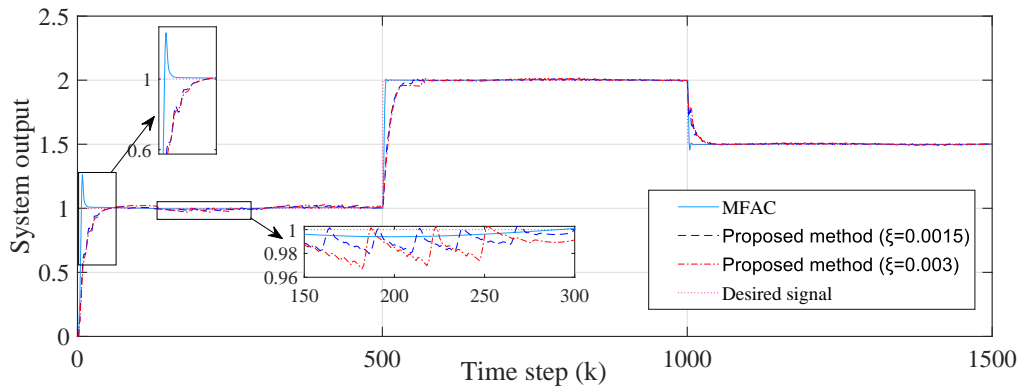
where $x_1(k) = 1 + 0.2 \sin(2k\pi/400)$, $x_2(k) = 0.5 + 0.2k/400$ and $x_3(k) = \exp(-k/400)$.

The preset reference signal is shown below:

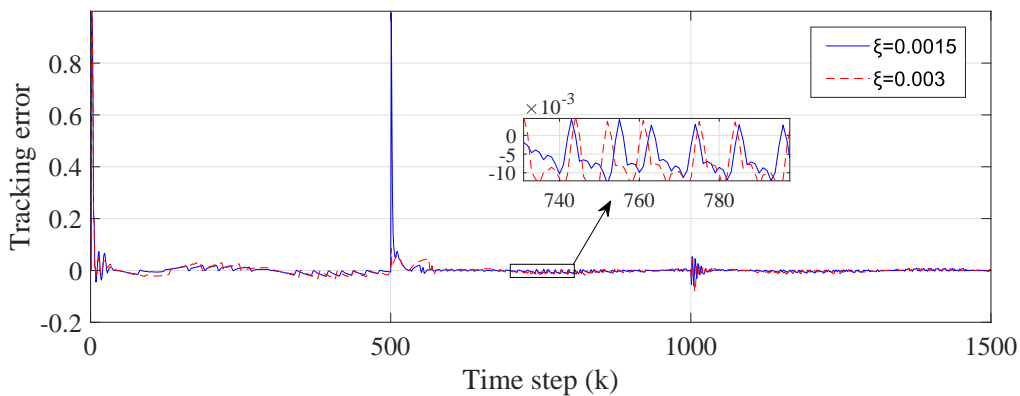
$$y^*(k) = \begin{cases} 1, & k \leq 500 \\ 2, & 500 < k \leq 1000 \\ 1.5, & 1000 < k \leq 1500 \end{cases} \quad (31)$$

The parameters for this simulation are set as follows. $\hat{\phi}(1) = 4.3$, $K_o = 0.05$, $\mu = 1.8$, $\varepsilon = 0.001$, $\lambda = 100$, $\sigma = 1e - 4$, $\beta = 0.9$, $\omega = 0.5$, $K_f = 0.5$, $T_s = 1$. As for the event-triggered parameter ξ , two values are set for comparison: $\xi = 0.0015$ and $\xi = 0.003$. The results of our simulation example are shown in Figures 1-4 and Table 1.

The tracking performance is shown in Figure 1. Since the event-triggered control only updates the control signal at the event-triggered time, the tracking performance is not as good as the traditional MFAC method. In addition, due to the fact that the rate of the



(a) System output



(b) System output tracking error

FIGURE 1. Tracking performance

control signal is limited, the rapidity of the proposed method is slightly worse than that of the MFAC method. Because of this, the proposed method has no overshoot.

The system control input $u(k)$ is shown in Figure 2(a). Clearly, the system control input remains unchanged during the event-triggered times $k \in (k_i, k_{i+1})$, but the control signal of MFAC is always updated. Figure 3(a) shows the event-triggered times by the values of $\gamma(k)$ when $\xi = 0.0015$. Statistics of the number of event-triggered instants are shown in Table 1. The controller only executed 777 times in 1500 sampling instants, which saves 48% calculations for the controller. It is obvious that the event-triggered mechanism could reduce computation for the system.

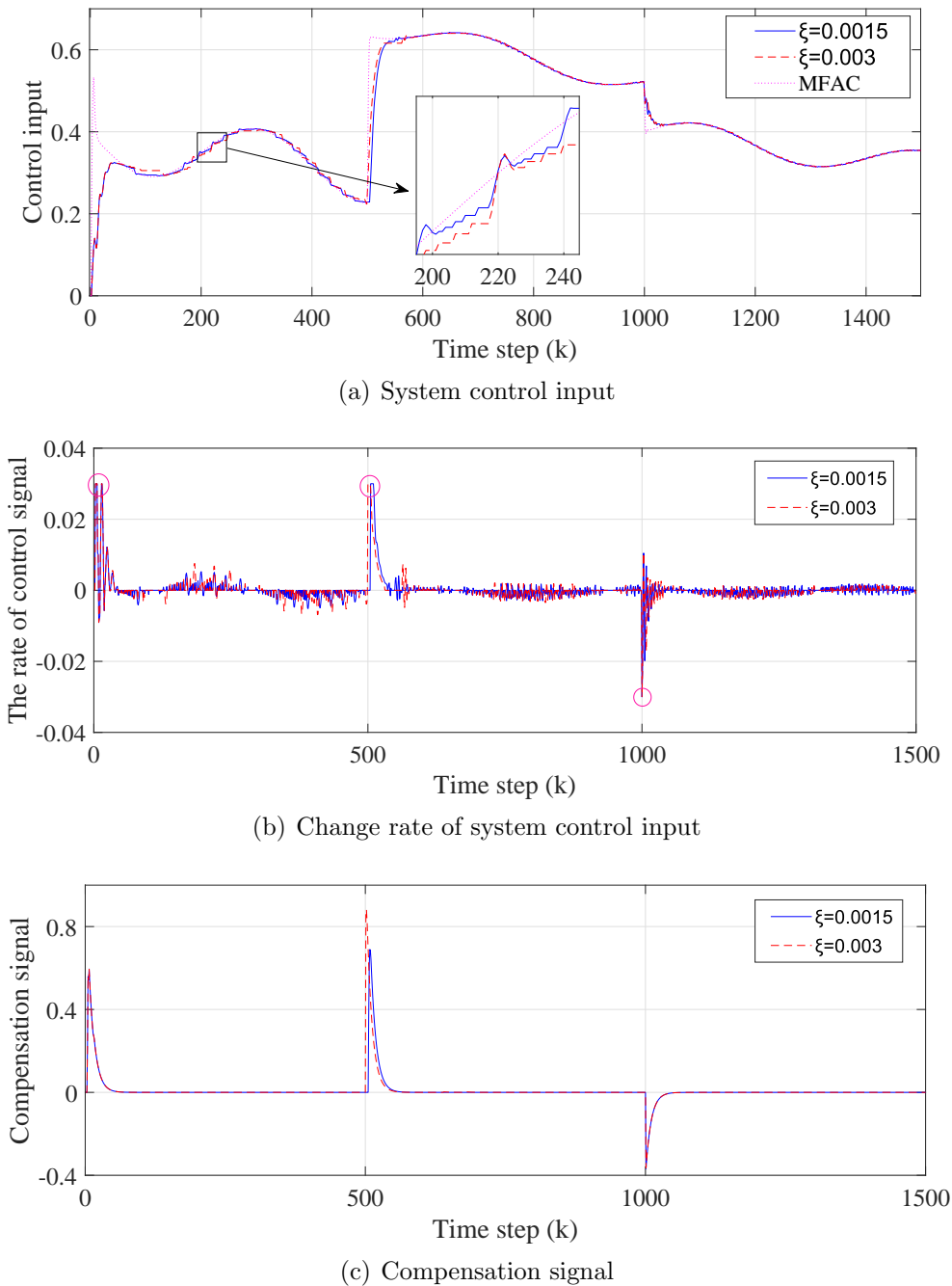


FIGURE 2. Control input and compensation signal

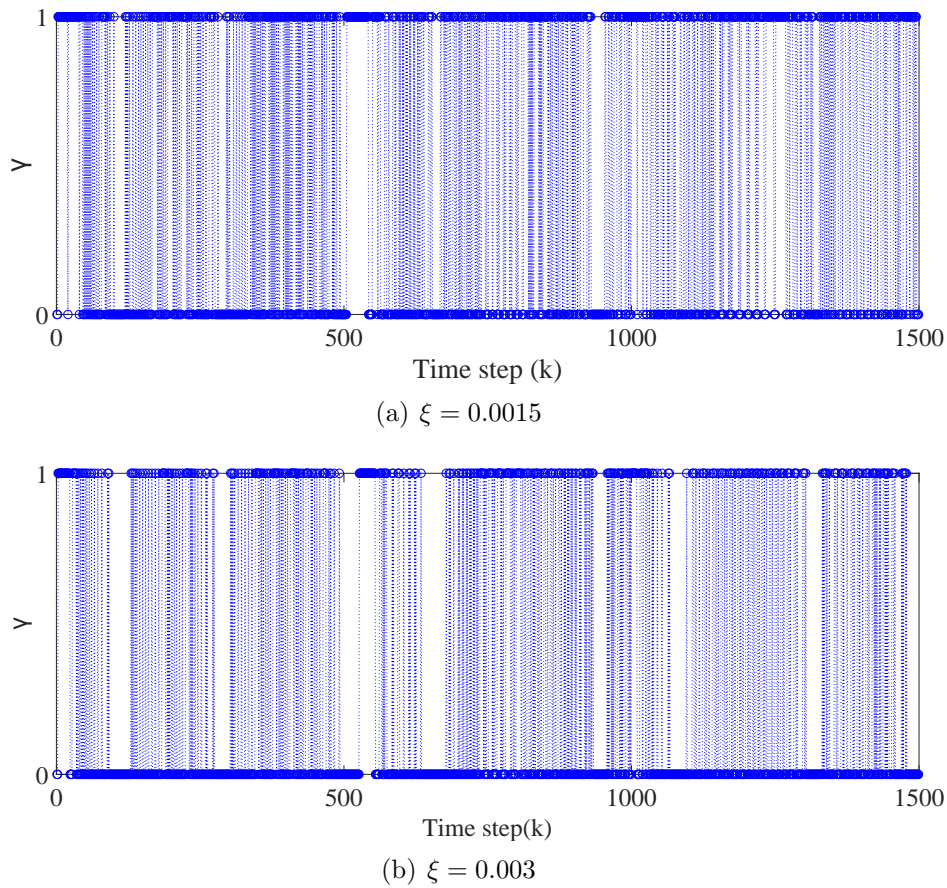


FIGURE 3. Event-triggered instants

TABLE 1. The number of trigger times

ξ	0.0015	0.003
Trigger times	777	533

The simulation results of $\tilde{u}(k)$ and $\theta(k)$ are shown in Figure 2(b) and Figure 2(c) respectively. When $\tilde{u}(k)$ is in the limited state (the parts marked with circles in the figure), the compensation signal will make compensation immediately, so as to guarantee the accuracy of output tracking and avoid saturation phenomenon.

Figure 4 shows the change curve of PPD parameter estimation. Obviously, the change of PPD estimation satisfies the reset mechanism in Remark 2.1.

Furthermore, in order to reflect the influence of event trigger parameters on the system and controller, we change the event-triggered parameter to $\xi = 0.003$, and keep other parameters unchanged. Comparing the results in Figure 1(a) and Figure 1(b) when the ξ changes to 0.003 from 0.0015, the performance is little worse when the system is in steady state. The event-triggered instants are shown in Figure 3(b). The total amount of event-triggered times is 533 during the 1500 sampling times. The percentage of calculation saved for the controller reaches 64%. It can also be seen from Figure 2(a) and Table 1 that the number of triggers is less than $\xi = 0.0015$.

Comparing with the results when $\xi = 0.0015$, it can be concluded that when the parameter ξ becomes larger, the control performance will become a little worse, but the number of event triggers times will be reduced accordingly. Therefore, the calculation

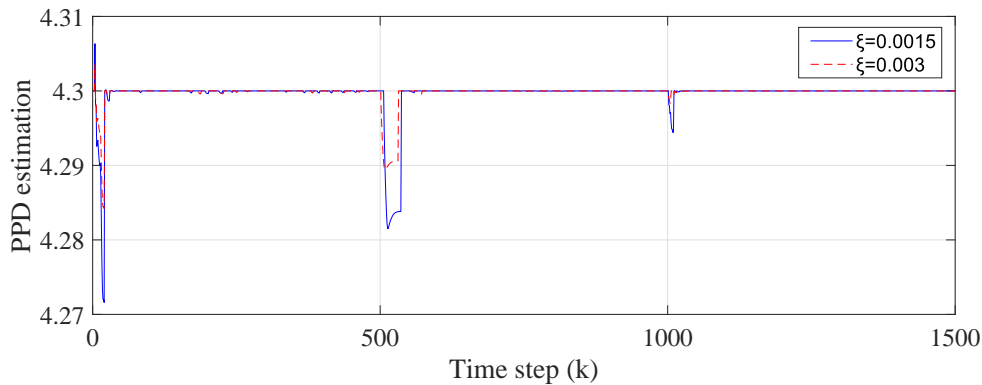


FIGURE 4. PPD estimation $\hat{\phi}(k)$

amount and control performance can be balanced by adjusting this parameter to achieve the expected control effect.

The above analysis shows that the simulation results are consistent with the theory, so one can conclude that the proposed method not only can ensure the control performance but also significantly reduces the computational burden.

5. Conclusion. In this paper, a model-free adaptive event-triggered sliding mode constrained control strategy is proposed. The linearized data-driven model of the discrete-time SISO nonlinear system is constructed via the CFDL technique and observer-based estimation algorithm, which solves the modeling problems for systems with complex dynamics. Besides, the actuator saturation problem is solved by adding the anti-windup compensator. In addition, the proposed control strategy only updates the control signal when the trigger condition is satisfied, which not only ensures the tracking performance, but also reduces the computational burden. The proposed control strategy is verified suitable for many industrial systems with limited computing resources by stability proof and simulation examples.

The ETC mechanism designed in this paper is fixed threshold type; in future research, a relative threshold type mechanism is expected based on the proposed strategy.

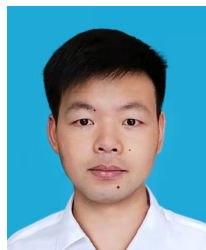
Acknowledgment. This work is partially supported by the National Natural Science Foundation of China (61973140). The authors also appreciatively acknowledge the helpful suggestions and comments of the reviewers, which have enhanced the presentation.

REFERENCES

- [1] Z. Hou and S. Jin, *Model Free Adaptive Control: Theory and Applications*, Kluwer Academic Publishers, Boston, 2003.
- [2] D. Xu, B. Jiang and P. Shi, Adaptive observer based data-driven control for nonlinear discrete-time processes, *IEEE Transactions on Automation Science and Engineering*, vol.11, no.4, pp.1037-1045, 2013.
- [3] D. Xu, Y. Shi and Z. Ji, Model free adaptive discrete-time integral sliding mode constrained control for autonomous 4WMV parking systems, *IEEE Transactions on Industrial Electronics*, vol.65, no.1, pp.834-843, 2017.
- [4] Z. Hou and S. Jin, A novel data-driven control approach for a class of discrete-time nonlinear systems, *IEEE Transactions on Control Systems Technology*, vol.19, no.6, pp.1549-1558, 2010.
- [5] X. Bu, Z. Hou and H. Zhang, Data-driven multiagent systems consensus tracking using model free adaptive control, *IEEE Transactions on Neural Networks and Learning Systems*, vol.29, no.5, pp.1514-1524, 2018.

- [6] X. Shi, Y. Cao, Y. Li, J. Ma, S. Mohammad, X. Wu and Z. Li, Data-driven model-free adaptive damping control with unknown control direction for wind farms, *International Journal of Electrical Power & Energy Systems*, vol.123, 2020.
- [7] Z. Hou and Z. Wang, From model-based control to data-driven control: Survey, classification and perspective, *Information Sciences*, vol.235, pp.3-35, 2013.
- [8] D. Xu, B. Jiang and P. Shi, A novel model-free adaptive control design for multivariable industrial processes, *IEEE Transactions on Industrial Electronics*, vol.61, no.11, pp.6393-6398, 2014.
- [9] D. Xu, X. Song, B. Jiang, W. Yang and W. Yan, Data-driven sliding mode control for MIMO systems and its application on linear induction motors, *International Journal of Control, Automation and Systems*, vol.17, no.7, pp.1717-1725, 2019.
- [10] Z. Wang, Adaptive fuzzy system compensation based model-free control for steer-by-wire systems with uncertainty, *International Journal of Innovative Computing, Information and Control*, vol.17, no.1, pp.141-152, 2021.
- [11] X. Wang, X. Li, J. Wang, X. Fang and X. Zhu, Data-driven model-free adaptive sliding mode control for the multi degree-of-freedom robotic exoskeleton, *Information Sciences*, vol.327, pp.246-257, 2016.
- [12] N. Lin, R. Chi and B. Huang, Event-triggered model-free adaptive control, *IEEE Transactions on Systems, Man, and Cybernetics: Systems*, vol.51, no.6, pp.3358-3369, 2021.
- [13] D. Liu and G. Yang, Neural network-based event-triggered MFAC for nonlinear discrete-time processes, *Neurocomputing*, vol.272, pp.356-364, 2018.
- [14] D. Liu and G. Yang, Event-based model-free adaptive control for discrete-time non-linear processes, *IET Control Theory & Applications*, vol.11, no.15, pp.2531-2538, 2017.
- [15] A. Wang, L. Liu and J. Qiu, Event-triggered robust adaptive fuzzy control for a class of nonlinear systems, *IEEE Transactions on Fuzzy Systems*, vol.27, no.8, pp.1648-1658, 2019.
- [16] H. Li, Y. Wang and H. Zhang, Data-driven-based event-triggered tracking control for non-linear systems with unknown disturbance, *NIET Control Theory & Applications*, vol.13, no.14, pp.2197-2206, 2019.
- [17] Y. Zhang, L. Zou and B. Song, Event-triggered model-free adaptive control of networked nonlinear systems with packet dropouts compensation, *2019 Chinese Automation Congress (CAC)*, pp.2101-2106, 2019.
- [18] C. Xi and J. Dong, Adaptive fuzzy guaranteed performance control for uncertain nonlinear systems with event-triggered input, *Applied Mathematics and Computation*, vol.363, 2019.
- [19] L. Liu, X. Li, Y. Liu and S. Tong, Neural network based adaptive event trigger control for a class of electromagnetic suspension systems, *Control Engineering Practice*, vol.106, 2021.
- [20] J. S. V. S. Kumar and P. M. Rao, Sliding mode control of interleaved double dual boost converter for electric vehicles and renewable energy conversion, *ICIC Express Letters*, vol.14, no.2, pp.179-188, DOI: <https://doi.org/10.24507/icicel.14.02.179>, 2020.
- [21] W. Zhang, D. Xu, B. Jiang and T. Pan, Prescribed performance based model-free adaptive sliding mode constrained control for a class of nonlinear systems, *Information Sciences*, vol.544, pp.97-116, 2021.
- [22] T. Sophie and T. Matthew, Anti-windup design: An overview of some recent advances and open problems, *IET Control Theory & Applications*, vol.3, no.1, pp.1-19, 2009.
- [23] J. T. Spooner, M. Maggiore, R. Ordóñez and K. M. Passino, *Stable Adaptive Control and Estimation for Nonlinear Systems: Neural and Fuzzy Approximator Techniques*, Wiley, New York, 2002.

Author Biography



Chuanwen Gao received the B.S. degree in electrical engineering and automation from China University of Mining and Technology, Xuzhou, China, 2017. He is currently working toward the M.S. degree in electrical engineering with Jiangnan University, Wuxi, China.

His current research interests include model-free adaptive control and event-triggered control.



Weiming Zhang received his M.S. degree in control engineering from Jiangnan University, Wuxi, China in 2020. He is currently working toward the Ph.D. degree in control science and engineering with Jiangnan University, Wuxi, China.

His current research interests include data-driven control, model-free adaptive control and multi-agent systems.



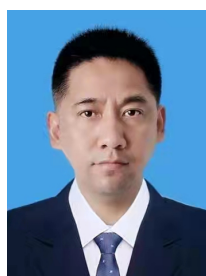
Dezhi Xu received the Ph.D. degree in control theory and control engineering from Nanjing University of Aeronautics and Astronautics, China, in 2013.

Dr. Xu was a Visiting Fellow with the Department of Biomedical Engineering, City University of Hong Kong, Hong Kong, from 2018 to 2019. He joined Jiangnan University from 2014, as an Associate Professor. His current research interests include data driven control, fault diagnosis and fault-tolerant control, multi-agent systems and CPSs, technologies of renewable energy, motor control, and smart grid. Dr. Xu was a recipient of the First Class Award of Science and Technology Progression from the China General Chamber of Commerce in 2016 for his research results. He is a Committee Member of the Association of Energy Internet, and Trusted Control of the Chinese Association of Automation (CAA), and Committee Member of Energy Storage of the China Renewable Energy Society (CRES).



Weilin Yang received his B.Eng. degree in machine design & manufacture and their automation from University of Science and Technology of China, Hefei, China, in 2009, and the Ph.D. degree in mechanical engineering from City University of Hong Kong, Hong Kong SAR in 2013.

Dr. Yang was a postdoctoral researcher at Masdar Institute of Science and Technology (now Khalifa University), Abu Dhabi, UAE, 2013-2016. He was a research engineer of General Electric (GE) Global Research, Shanghai, 2016-2017. He joined Jiangnan University in July 2017, where he is currently an Associate Professor. His research interests include modeling and control of energy systems, robust model predictive control, and data-driven control.



Tinglong Pan received his B.Eng. degree in industrial automation from China University of Mining and Technology, Xuzhou, China, in 1999, and the Ph.D. degree in power electronics and power drive from China University of Mining and Technology, Xuzhou, China, in 2004.

Dr. Pan is currently a Professor at Jiangnan University, where his research interests include microgrid control technology, power conversion technology, power drive system and its intelligent control technology.